J Mater Sci: Mater Med (2010) 21:1959–1968
DOI 10.1007/s10856-010-4057-x

In vitro biocompatibility and corrosion resistance of a new implant titanium base alloy

E. Vasilescu · P. Drob · D. Raducanu · V. D. Cojocaru · I. Cinca · D. Iordachescu · R. Ion · M. Popa · C. Vasilescu

Received: 9 July 2009 / Accepted: 11 March 2010 / Published online: 25 March 2010

Abstract One objective of this work was to study the corrosion resistance of the new implant Ti–10Zr–5Ta–5Nb alloy in physiological fluids of different pH values, simulating the extreme functional conditions. Another objective was in vitro biocompatibility evaluation of the new alloy using human fetal osteoblast cell line hFOB 1.19. Cytocompatibility was assessed by determination of possible material cytotoxic effects, cell morphology and cell adhesion. The thermo-mechanical processing of the new implant alloy consisted in plastic deformation (almost 90%) performed by hot rolling accompanied by an initial and final heat treatment. The new Ti–10Zr–5Ta–5Nb alloy presented self-passivation, with a large passive potential range and low passive current densities, namely, a very good anticorrosive resistance in Ringer solution of acid, neutral and alkaline pH values. Cell viability was not affected by the alloy substrate presence and a very good compatibility was noticed.

1 Introduction

In the last years, researches upon cytocompatibility were focused on the primary mechanisms which control the cellular behaviour. As regarding bio-non bio interactions, in the first stage, the cell adhesion take place, followed by the cell spreading and proliferation on the artificial substrate [1–5]. The quality of first stage cell-artificial material interactions clearly influences the cell proliferation and differentiation [3]. The molecules responsible for these processes are represented by integrin receptors and cytoskeletal components [6]. Integrins are extracellular matrix receptors involved in relaying the extracellular signals inside the cell through focal adhesions, thus influencing nuclear gene expression and implicitly extracellular matrix (ECM) biosynthesis by fibronectine network formation and specific proteins incorporation [7, 8].

In the last time, the type β titanium alloys (containing Ti, Ta, Nb, Zr) are very attractive for biomedical applications because their very high mechanical resistance (1.6 GPa), very important for orthopaedic implants and low elasticity modulus (60–80 GPa), very closed with of the bone (40 GPa). In addition, the β stabilising elements as Nb, Ta, and Zr are very resistant and biocompatible [9–19].

Studies concerning the metal biocompatibility [20–22] show that Ti, Ta, Nb and Zr have an excellent cytocompatibility and much reduced cytotoxic effects for short and long term.

Also, the metal toxicity depends by the reactivity of the released ions to proteins and by the primary stability of the corrosion products and oxides existing or resulted after their interactions with the bone and the surrounding tissues [20, 23–29].

In the case of an implant surgery, local acidity of the physiological fluid can appear immediately after surgical application, due to the hydrolysis of the passivation and corrosion products or in the zones with low oxygen content [30] or local alkalinity can appear in the ill periods or in the case of inflammations and infections [31]. Taking into

E. Vasilescu (✉) · P. Drob · M. Popa · C. Vasilescu
Institute of Physical Chemistry "Ilie Murgulescu", Spl. Independentei 202, Bucharest 060021, Romania
e-mail: ec_vasilescu@yahoo.com

D. Raducanu · V. D. Cojocaru · I. Cinca
Faculty of Material Science and Engineering, Politehnica University, Spl. Independentei 313, Bucharest 060042, Romania

D. Iordachescu · R. Ion
Department of Biochemistry and Molecular Biology, Bucharest University, Spl. Independentei 93, Bucharest 050095, Romania

account the complexity of the human body, were simulated various conditions that can appear for "long term service life" of an implant by the using of Ringer solution of different pH values (2.33, 7.1, 9.1) [32, 33].

Non-uniformity of the pH along the surface of an implant can generate potential gradients ΔE_{oc}(pH) that can accelerate the corrosion and for this reason, these potential gradients were simulated and determined [32–35].

A new, complex base titanium alloy, Ti-Zr-Nb-Ta type, with non-toxic alloying elements was realized to be used in implantology. It does not contain alloying elements which can determine inflammations and/or osteolysis as Al or V [25, 29]. New obtained Ti-10Zr-5Nb-5Ta alloy was processed further by plastic deformation and heat treatments.

One objective of this work was to study the corrosion resistance of the new implant Ti-–10Zr–5Ta–5Nb alloy in artificial physiological fluids (of different pH values-simulating the extreme functional conditions) as an aspect of its compatibility. The second objective was in vitro cytocompatibility evaluation of the new Ti–10Zr–5Ta–5Nb alloy using human fetal osteoblast cell line hFOB 1.19. This was assessed by measuring potential cytotoxic effects and by fluorescence microscopic studies regarding cell morphology and cell adhesion.

2 Materials and methods

2.1 Alloy obtaining

First was established the alloy chemical composition taking into account the final biomaterial characteristics [36–40]. The obtaining method and laboratory technology for the synthesis of Ti–10Zr–5Ta–5Nb_c alloy (in casting state) was settled by experimental researches. An electron beam furnace type EMO 80, with an installed power of 80 kW was used. The alloy synthesis was performed in two steps under vacuum, consisting in melting and re-melting both with cooling stages inside furnace.

The realised chemical composition in weight % is: Zr—9.12, Nb—4.09, Ta—4.16, Fe—0.036, O_2—0.195, N_2—0.004, H_2—0.0016, Ti-balance.

The thermo-mechanical processing of the new realised alloy Ti–10Zr–5Ta–5Nb_{tt} consists in plastic deformation performed by hot rolling accompanied by an initial and final heat treatment. The initial heat treatment was realized to homogenize the casting structure and consists in heating at 1000°C for 2 h followed by water cooling. Final heat treatment (heating at 1000°C for 1 h followed by furnace cooling) was applied in order to obtain structural transformation associated with various mechanical and corrosion behaviour. Both heat treatments were performed using an electrical laboratory furnace. Between the initial and final heat treatment, a plastic deformation process was placed following the idea to show the alloy capacity to be plastically deformed. The plastic deformation process was realized at 1000°C using a laboratory roll-mill (cylinder diameter: 150 mm, rolling mill power: 45 kW, rolling mill speed: 1.5 m/s) in 16 steps and was finished in good condition, this meaning no lateral cracks, surface defects and material discontinuities were present. The total deformation degree realized was almost 90% which indicates a good workability of the new alloy.

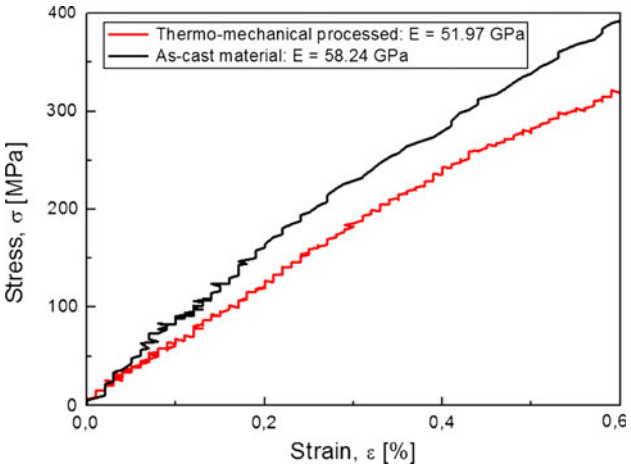

Fig. 1 Strain–stress diagram for as-cast and thermo-mechanical processed Ti–10Zr–5Ta–5Nb alloy

As observed in Fig. 1 the calculated value for elastic modulus is situated to 58.24 GPa for as-cast material and 51.97 GPa for thermo-mechanical processed material, showing a decreasing in elastic modulus of about 10.76% as an effect of the thermo-mechanical processing. Obtained elastic modulus is situated much more close to cortical bone elastic modulus (max. 35 GPa), reducing the risk of bone resorption [41].

2.2 Electrochemical measurements

The electrodes for electrochemical and in vitro experiments were grinded with metallographic paper of different granulations to a mirror surface. Then, for electrochemical measurements, the electrodes were fixed in a Stern–Makrides hold system, rinsed with distilled water, degreased in boiling benzene and dried.

All electrochemical measurements were carried out in Ringer solution of pH = 2.33 (obtained by HCl addition), pH = 7.1 (normal pH), pH = 9.1 (obtained by KOH

addition). The composition of Ringer solution was (g/l): NaCl—6.8, KCl—0.4, $CaCl_2$—0.2, $MgSO_4 \cdot 7H_2O$—0.2048, $NaH_2PO_4 \cdot H_2O$—0.1438, $NaHCO_3$—1.1, glucose-1.

The temperature was kept at 37 ± 1°C

Electrochemical glass cell was provided with inlets for the working electrode, for the auxiliary platinum electrode and for Haber-Luggin capillary connected with the reference saturated calomel electrode (SCE).

The following experimental techniques were used: potentiodynamic and linear polarization and monitoring of the open circuit potentials [42], E_{oc} and corresponding open circuit potential gradients, $\Delta E_{oc}(pH)$ (due to the pH non-uniformities of the Ringer solution) versus exposure time (750 h).

The cyclic potentiodynamic polarization [43] was applied beginning from −0.5 to +4.0 V (vs. SCE) using a scan rate of 10 mV/s. Voltalab 80 equipment with its VoltaMaster 4 program were used. From the voltammograms, the main electrochemical parameters were determined: E_{corr}—corrosion potential, like zero current potential, E_p—passivation potential at which the current density is constant; $|E_{corr} - E_p|$ difference represents the tendency to passivation (low values characterise a good, easy passivation); ΔE_p—passive potential range of the constant current; i_p—passive current density.

If the reverse curve presents lower currents than the direct curve, it results a very stable passive state. If the reverse curve shows higher currents than the direct curve, pitting corrosion exists.

The linear polarization measurements (Tafel) were applied for a range of ±200 mV around the open circuit potential, with a scan rate of 10 mV/sec. The same Voltalab 80 equipment with its VoltaMaster 4 program that delivered the values of the corrosion current densities (i_{corr}) and rates (V_{corr}) obtained from Tafel curves was used.

The total quantity of the ions (ng/cm^2) released in the solution was determined:

$$\text{ion release rate} = 1.016.V_{corr} \times 10^5 \quad (1)$$

where: V_{corr} = corrosion rate in mm/year.

The open circuit potentials E_{oc} were monitored with the exposure time (750 exposure hours till present) using a performing Hullett-Pakard multimeter.

The following open circuit potential gradients that could appear due to the pH non-uniformities along the metal surface were simulated:

$$\Delta E_{oc1}(pH) = E_{oc}^{pH=2.33} - E_{oc}^{pH=7.1} \quad (2)$$

$$\Delta E_{oc2}(pH) = E_{oc}^{pH=2.33} - E_{oc}^{pH=9.1} \quad (3)$$

$$\Delta E_{oc3}(pH) = E_{oc}^{pH=7.1} - E_{oc}^{pH=9.1} \quad (4)$$

2.3 Cytocompatibility measurements

2.3.1 Osteoblast cell culture

Human fetal osteoblasts (hFOB 1.19, purchased from American type cell culture collection) were cultured in DMEM (dulbecco's modified eagle's medium)-Ham's F-12 1:1 media (Sigma–Aldrich) supplemented with 10% fetal bovine serum (FBS, Gibco) and 0.3 mg/ml G 418 antibiotic on tissue culture polystyrene (TCPS) plates and incubated at 34°C in a standard incubator with 5%CO_2 in air. Cells were plated at the same density (1.2×10^4 cells/cm^2) on tissue culture polystyrene plates (which served as positive control) and test metal. Prior to cell culture, test material was sterilized at 180°C for 30 min. Cells were allowed to adhere and to proliferate for specific times, with media changed every 3 days.

2.3.2 Assay of cytotoxic material potential

Human fetal osteoblast, hFOB 1.19 cells were seeded onto TCPS and alloy surfaces and incubated over a period of 3 days under standard cell culture conditions. Samples of 100 µl culture media were taken after 24, 48 and 72 h and a lactate dehydrogenase (LDH) test was performed with a Cytotoxicity Detection Kit from Sigma (TOX-7) according to the manufacturer's protocol.

2.3.3 Immunocitochemical staining of actin and fibronectin

Cell morphology on test material was assessed by fluorescent staining of actin. After culturing for 1, 4 and 24 h, cells were washed with phosphate buffer saline (PBS) three times and fixed with 4% paraformaldehyde for 10 min. Fixed cells were rinsed with PBS and permeabilized for 15 min with 0.1% Triton X-100 (Sigma) in PBS. Then, cells were pre-incubated for 1 h at room temperature with 2% bovine serum albumin (BSA, Sigma) to minimize non-specific protein–protein interactions. After blocking with BSA solution, cells were incubated for 1 h at 37°C with fluorescein isothiocyanate (FITC)-conjugated phalloidin for actin detection. For extracellular matrix protein analysis, cells were maintained in culture for 5 days after seeding. Immunostaining for fibronectin was achieved using a mouse anti-fibronectin monoclonal primary antibody (1:50 dilution) and a goat anti-mouse IgG FITC-conjugated secondary antibody (1:100 dilution) from Santa Cruz Biotechnology.

2.3.4 Statistical analysis

Data were expressed as mean value (MV) ± standard deviation (SD) of three independent experiments.

3 Results

3.1 Corrosion behaviour of Ti–10Zr–5Ta–5Nb alloy from electrochemical measurements

3.1.1 Corrosion behaviour of Ti–10Zr–5Ta–5Nb alloy in Ringer solution of pH = 2.33

From Fig. 2a it resulted that the thermo-mechanical processed Ti–10Zr–5Ta–5Nb_{tt} alloy had a self-passivation metal behaviour, without potential domain of active–passive dissolution and with a very large passive potential range (Table 1), as large as of the casting alloy (>4 V). Corrosion potential of treated alloy of −0.247 V (Table 1) is the most electropositive at this pH value and it is placed on the Pourbaix diagrams [44] in the passivation domain of Ti, Ta and Nb and in the corrosion domain of Zr. Also, the treated alloy presented the lowest value for $|E_{corr}-E_p|$ difference, showing the easiest tendency to passivation. The treated alloy has a relative low passive current density (in the domain of +0.4/0.5 V) of 20.5 μA/cm^2. In comparison with base metal and un-treated alloy (in casting state), it was observed the improvement of the main electrochemical parameters as result of the application of the thermo-mechanical treatment.

Table 1 Main electrochemical parameters in Ringer solution of different pH values, at 37°C

Material	E_{corr} (V)	E_p (V)	ΔE_p (V)	$\|E_{corr} - E_p\|$ (V)	i_p (μA/cm^2)
pH = 2.33					
Ti	−0.660	+0.30	>4	0.960	127
TiZrTaNb$_c$	−0.257	+0.25	>4	0.507	107
TiZrTaNb$_{tt}$	−0.247	+0.23	>4	0.477	20.5
pH = 7.1					
Ti	−0.480	+0.08	>4	0.560	96
TiZrTaNb$_c$	−0.507	+0.15	>4	0.657	30
TiZrTaNb$_{tt}$	−0.231	+0.10	>4	0.331	20
pH = 9.1					
Ti	−0.720	+0.50	>4	1.220	2180
TiZrTaNb$_c$	−0.373	+0.45	>4	0.823	102
TiZrTaNb$_{tt}$	−0.252	+0.25	>4	0.502	25

For thermo-mechanical treated alloy, from Tafel curves were obtained low corrosion rate of 2.08 μm/year and a reduced total quantity of ions released in physiological environment that places Ti–10Zr–5Ta–5Nb_{tt} alloy in resistance class "very stable" (Table 2). Because, the corrosion rate of un-treated alloy had higher values, it

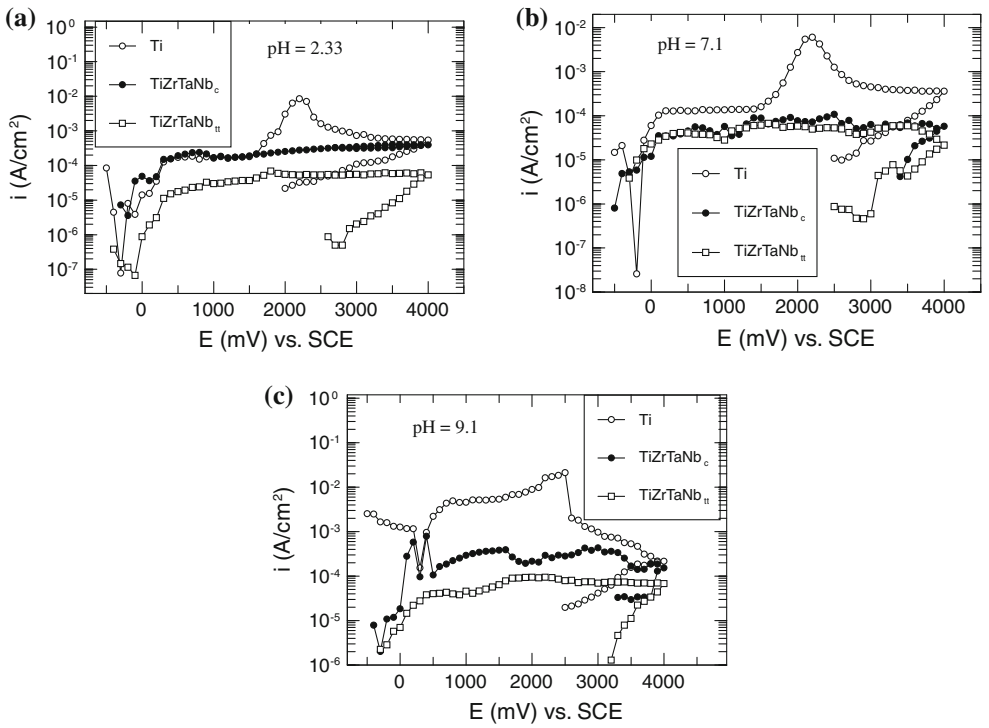

Fig. 2 Cyclic potentiodynamic curves at 37°C in Ringer solution of: **a** pH = 2.33, **b** pH = 7.1, **c** pH = 9

Table 2 Corrosion rates and ion release in Ringer solution of different pH values, at 37°C

Material	i_{corr} ($\mu A/cm^2$)	V_{corr} ($\mu m/yr$)	Category	Ion release ($\mu g/cm^2$)
pH = 2.33				
Ti	0.746	8.63	VS	0.88
$TiZrTaNb_c$	0.94	10.78	S	1.11
$TiZrTaNb_{tt}$	0.18	2.08	VS	0.21
pH = 7.1				
Ti	0.822	9.50	VS	0.97
$TiZrTaNb_c$	0.23	2.66	VS	0.27
$TiZrTaNb_{tt}$	0.10	1.16	VS	0.12
pH = 9.1				
Ti	1.19	13.76	S	1.40
$TiZrTaNb_c$	0.15	1.74	VS	0.18
$TiZrTaNb_{tt}$	0.11	1.27	VS	0.13

VS very stable, *S* stable

results that the thermo-mechanical treatment had a very favourable effect on this parameter.

3.1.2 *Corrosion behaviour of Ti–10Zr–5Ta–5Nb alloy in Ringer solution of pH = 7.1*

In normal Ringer solution of pH = 7.1, that usually exists in human body, the thermo-treated $Ti–10Zr–5Ta–5Nb_{tt}$ alloy is self-passivated (Fig. 2b), has a larger of +4 V passivation potential range (maximum limit of experiments) and a relative low passive current density of 20 $\mu A/cm^2$ (Table 1); the corrosion potential of −0.231 V shows that the all constituent elements are in the passive state on Pourbaix diagrams [44], so, the thermo-treated alloy is very resistant and passive. Also, the treated alloy presented the best value for the passivation potential, E_p and $|E_{corr} - E_p|$ difference, proving a very good and very easy tendency to passivation (Table 1). The positive effect of thermo-mechanical treatment of the ennobling of the corrosion potential, of the improvement of the tendency to passivation and of the decrease of the passive current (Table 1) is important.

Corrosion rate (Table 2) and corresponding ion release rate for thermo-treated $Ti–10Zr–5Ta–5Nb_{tt}$ alloy has low value, placing the alloy in "very stable" class.

3.1.3 *Corrosion behaviour of Ti–10Zr–5Ta–5Nb alloy in Ringer solution of pH = 9.1*

In alkaline Ringer solution of pH = 9.1, that can accidentally appear in the human body, the thermo-treated $Ti–10Zr–5Ta–5Nb_{tt}$ alloy presented also spontaneous passivation (Fig. 2c), having a very large passive potential range (> +4 V) and relative reduced passive current density of 25 $\mu A/cm^2$ (Table 1).

Taking into account the value of the corrosion potential of −0.252 V, from Pourbaix diagrams [44] it results that both the base metal Ti and the alloying elements Zr, Ta and Nb are in the passive state, so, the alloy is in the passive, stable, resistant state. Tendency to passivation has the best value for the treated alloy (Table 1).

The thermo-mechanical treatment leaded to a better behaviour of the treated alloy because all electrochemical parameters have better values than un-treated alloy.

From the Tafel curves for the thermo-mechanical treated alloy it resulted low values of the corrosion rates and ion release rate, in the "very stable" class (Table 2). A decrease of the corrosion rate of the treated alloy than of the casting alloy it resulted proving the favourable effects of the thermo-mechanical processing.

3.1.4 *Corrosion behaviour from monitoring of the open circuit potentials*

In Ringer solution of pH = 2.33, the variation in time of the open circuit potentials for the casting $Ti–10Zr–5Ta–5Nb_c$ alloy (Fig 3a) generally revealed their tendency to stabilize, the medium value after 750 exposure hours being about −0.240 V, a potential placed in the corrosion range of Zr and in the passive range of Ti, Ta and Nb in the Pourbaix diagrams [44]. The thermo-mechanical treated $Ti–10Zr–5Ta–5Nb_{tt}$ alloy presents slight more electropositive open circuit potentials (due to the positive influence of the applied treatments) with tendency to reach a constant level in time; the medium value of −0.200 V places Ti, Ta and Nb in the passive state and Zr in the corrosion state.

In normal Ringer solution of pH = 7.1 (Fig. 3b) it resulted more ennoble values of the E_{oc} both for casting and thermo-treated alloy, values which reaches −0.180 V, respectively −0.150 V, assuring a good stability and resistance, because the all alloying components are in the position of passive, stable state on the Pourbaix diagrams [44], at this pH value. It was observed that the treated alloy revealed more electropositive values of the E_{oc} potential than the casting alloy, as result of the beneficial effects produced by the thermo-mechanical treatment.

In alkaline Ringer solution of pH = 9.1 (Fig. 3c), the same phenomena were observed: more electropositive open circuit potentials in time (for casting alloy at ≈ −0.140 V and for treated alloy at ≈ −0.130 V), placed in the passive potential range for Ti, Zr, Ta and Nb, so, a stable state and good anticorrosive resistance; the thermo-mechanical treated alloy reveals the most electropositive values of the open circuit potentials because the heat

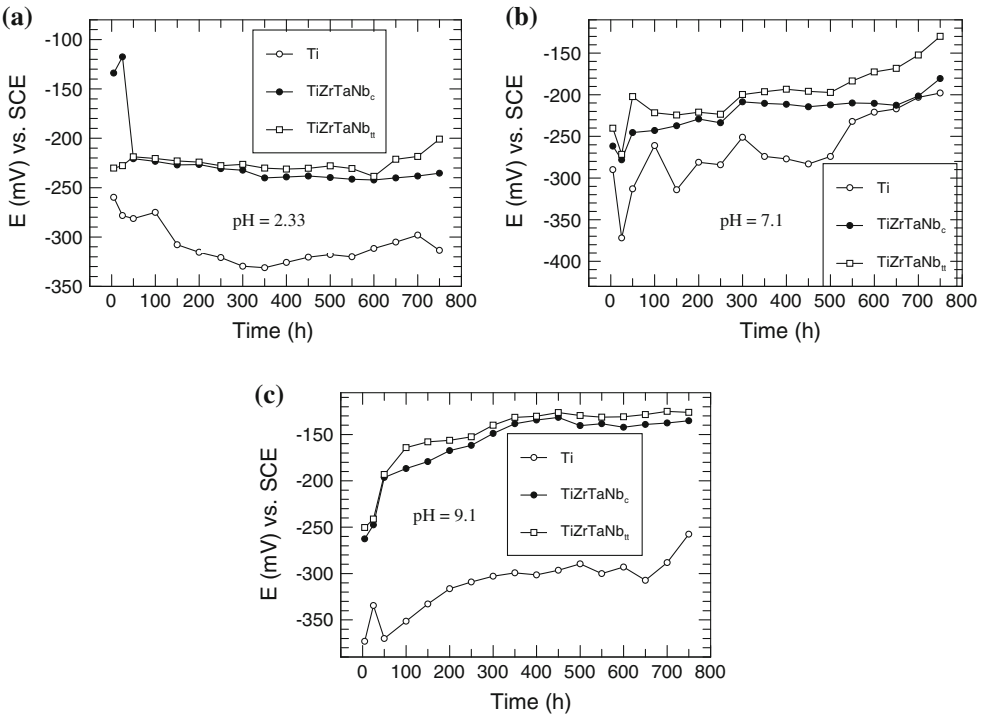

Fig. 3 Monitoring of the open circuit potentials in Ringer solution of: **a** pH = 2.33, **b** pH = 7.1, **c** pH = 9.1

treatment and plastic deformation processes took their effects to ennoble E_{oc}.

3.1.5 *Corrosion behaviour from the monitoring of the open circuit potential gradients*

From the long term monitoring of the open circuit potential gradients (Table 3) it resulted that for the casting Ti–10Zr–5Ta–5Nb$_c$ alloy, these gradients have low values (from 0.015 to 0.100 V), situated under the permitted limit of 0.6–0.7 V and can not generate galvanic or local corrosion [45–48].

Table 3 Open circuit potential gradients in Ringer solution, at 37°C

Material	Time (h)	ΔE_{oc1} (pH) (V)	ΔE_{oc2} (pH) (V)	ΔE_{oc3} (pH) (V)
Ti	100	−0.014	+0.077	+0.091
	300	−0.079	−0.027	+0.052
	500	−0.044	−0.028	+0.016
	750	−0.116	−0.056	+0.060
TiZrTaNb$_c$	100	+0.019	−0.037	−0.056
	300	−0.024	−0.083	−0.060
	500	−0.028	−0.099	−0.072
	750	−0.015	−0.100	−0.045
TiZrTaNb$_{tt}$	100	+0.001	−0.056	−0.057
	300	−0.027	−0.086	−0.060
	500	−0.031	−0.198	−0.068
	750	−0.071	−0.075	−0.004

In the case of thermo-mechanical treated Ti–10Zr–5Ta–5Nb$_{tt}$ alloy, it resulted very low values for open circuit potential gradients from 0.001 to 0.198 V (Table 3), that can not initiate and maintain galvanic cells or local corrosion.

3.2 In vitro biocompatibility assays

Comparative cell viability and cell morphology studies on osteoblasts grown on TCPS and new Ti–10Zr–5Ta–5Nb$_{tt}$ thermo-mechanical processed supports were performed.

3.2.1 *Ti–10Zr–5Ta–5Nb$_{tt}$ alloy effect on osteoblasts viability*

One of the objectives of this study was to determine if the new alloy affects the cellular survival. To test this parameter, the LDH activity in the culture media was measured. LDH is a soluble cytosolic enzyme that is released from the cells following loss of membrane integrity resulting from either apoptosis or necrosis. Therefore, LDH activity can be used as an indicator of cell membrane integrity and serves as a general mean to assess cytotoxicity. As shown in Fig. 4, the cell viability is lightly influenced by substrate presence [49–51]. Thus, after 24 h there is an increase of LDH activity in the culture media from osteoblasts seeded on Ti–10Zr–5Ta–5Nb$_{tt}$ alloy substrate compared with control specimen.

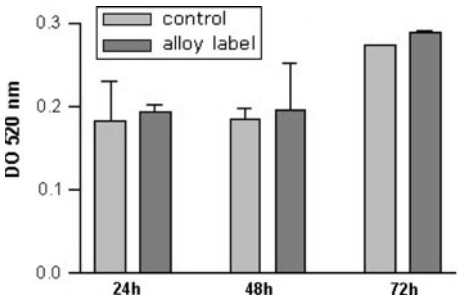

Fig. 4 Time course for the effect of Ti–10Zr–5Ta–5Nb_{tt} alloy on osteoblasts viability measured using LDH assay

3.2.2 *Cytomorphology and hFOB 1.19 cells orientation in contact with substrate*

The observation in fluorescent microscopy of osteoblasts grown on Ti–10Zr–5Ta–5Nb_{tt} substrate and on TCPS showed similarities regarding cell adhesion and density and spreading pattern (Fig. 5). The cells, initially having a round shape as a result of weak cellular contacts with the substrate, changed their morphology in time. Therefore, at 4 h post-seeding, the majority of hFOB 1.19 cells adopted an elongated morphology following their spreading.

3.2.3 *Osteoblast adhesion capacity on Ti–10Zr–5Ta–5Nb_{tt} alloy substrate*

Cells growth on the different substrates is favoured by secreted extracellular matrix (ECM) proteins. These ECM proteins in turn transduce extracellular signals, through the membrane receptors to the cytosol via focal contacts [52, 53].Variations in substratum surface properties affect cell–biomaterial interfacial characteristics, potentially influencing cellular functions. We examined the effect of Ti–10Zr–5Ta–5Nb_{tt} alloy on osteoblastic cell fibronectin synthesis. Fibronectin plays a major role in the adhesion of many cell types. The extent of cell adhesion in vitro is related not only to the ability of the cells to interact with matrix-bound fibronectin, when it is present, but also to the synthesis of fibronectin by the cells. Fibronectin expression by hFOB 1.19 grown on Ti–10Zr–5Ta–5Nb_{tt} alloy substrate and on TCPS is illustrated in Fig. 6. In both cases, a high fibronectin expression was noticed. However, differences in the fibronectin network distribution were remarked, probably as a result of surface topographic characteristics [54]. Thus, the fluorescent images showed a random fibronectin distribution on the control sample while on Ti–10Zr–5Ta–5Nb_{tt} alloy specimen, a more uniform fibronectin network was observed. One can conclude that both, control and tested material substrates revealed favourable adhesion properties for tested cells.

4 Discussions

The new alloy in casting state Ti–10Zr–5Ta–5Nb_c exhibited better corrosion potentials than the base metal in Ringer solutions of different pH values (Table 1) due to the galvanic couple effects of the alloying elements. Also, the thermo-mechanical treated alloy Ti–10Zr–5Ta-–5Nb_{tt} presented an improvement of its corrosion potentials in comparison with the casting alloy Ti–10Zr–5Ta–5Nb_c (Table 1) proving the beneficial effects of the thermo-mechanical processing.

The tendency to passivation $|E_{corr} - E_p|$ is better for casting alloy and is the best for thermo-mechanical treated alloy (Table 1), showing that the alloy can be easier passivated due to the favourable influence of the alloying elements that participate with their passive oxides (ZrO_2, Ta_2O_5, Nb_2O_5) [20, 55] to the formation of the passive layer. This layer is more compact, more stable than of the base metal, as it results from the lower values of the corrosion current densities and corrosion rates and corresponding ion release rates (Table 2).

Concerning the monitoring of the open circuit potentials in acid Ringer solution of pH = 2.33, the initial decrease of the E_{oc} values suggests the dissolution of the air-formed oxide film and their subsequent increase denotes the formation of a new passive oxide film in solution. It is known, that the passive layer on titanium and its alloys can be disrupted and it can get re-formed very easily, leading to spontaneous repassivation [56]. In normal Ringer solution of pH = 7.1, the ennoblement of the open circuit potentials indicates the increasing of the passive film thickness [57]. In alkaline Ringer solution of pH = 9.1, also, the same processes of the thickening of the passive layer take place.

Osteoblast viability increased on the thermo-treated alloy substrate than on the control specimen, the difference expressed in percents varying with observation time: 5.2% after 24 h, 5.95% after 48 h and 5.66% after 72 h, suggesting a better cytocompatibility for the alloy.

Regarding the hFOB 1.19 cells cytomorphology, after 24 h of culture, the cells displayed a quasi-similar polygonal shape with short cytoplasmic prolongations but slight differences in the distribution pattern. Thus, on the control sample, osteoblasts showed a network-like distribution, while on the Ti–10Zr–5Ta–5Nb_{tt} substrate, they tended to make parallel alignments as a result of contact guidance cue.

The osteoblast adhesion on the alloy substrate revealed a more uniform, parallel distribution than on the control sample, due to the more favourable topographic characteristics.

So, we had demonstrated that the new thermo-treated alloy Ti–10Zr–5Ta–5Nb_{tt} has a very good cytocompatibility.

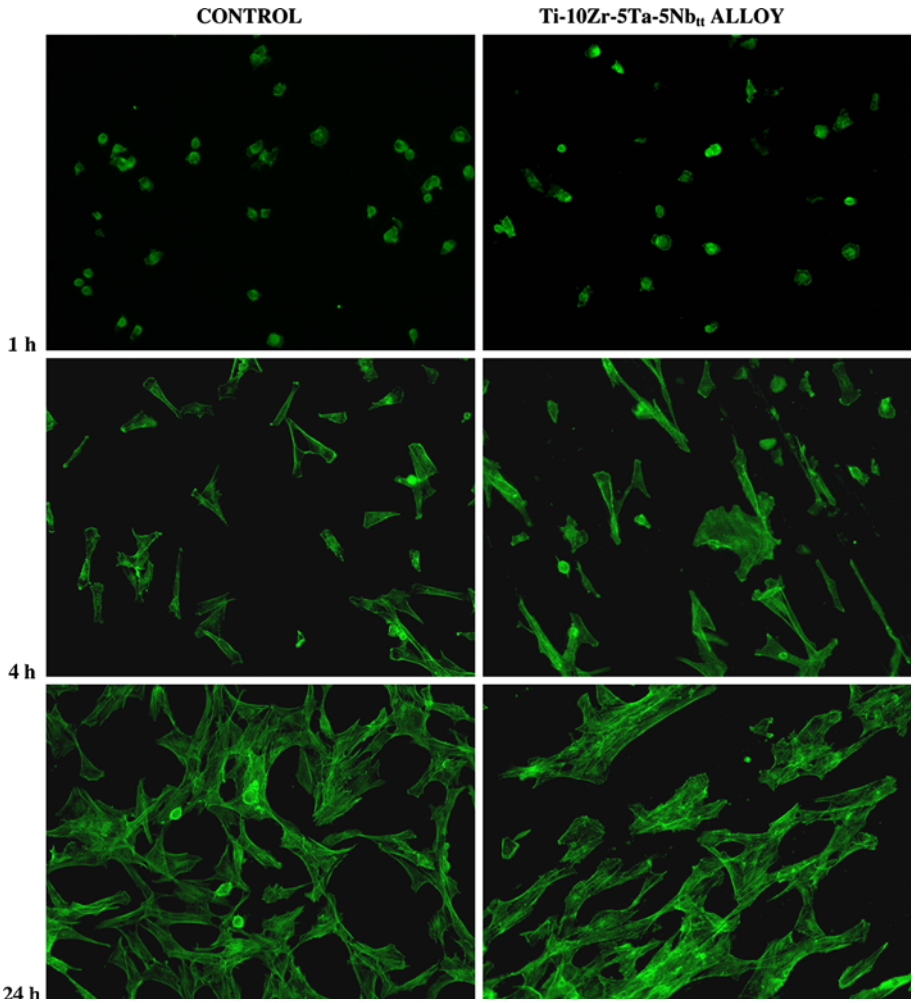

Fig. 5 Fluorescent images of hFOB 1.19 cells stained for actin on control specimen and on tested material (original magnitude 10x)

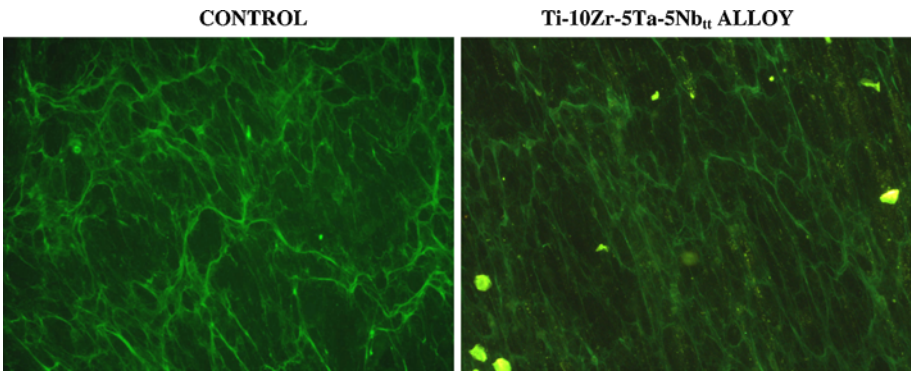

Fig. 6 Fibronectine fluorescence detection in hFOB 1.19 cells cultured on control sample and Ti–10Zr–5Ta–5Nb$_{tt}$ alloy specimen

5 Conclusions

1. Thermo-mechanical treated Ti–10Zr–5Ta–5Nb$_{tt}$ alloy exhibited a behaviour of self-passivation metal, with a large passive potential range and low passive current densities, namely, a very good anticorrosive resistance in Ringer solution of acid, neutral and alkaline pH values. The best behaviour was registered in neutral Ringer solution.
2. In comparison with the un-treated alloy, it appears an improvement of all electrochemical parameters and of the corrosion rates as result of the application of the thermo-mechanical treatment.
3. Cell viability is not affected by the alloy substrate presence, on the contrary it is increased.
4. Cell adhesion behaviour reflected by fibronectin expression on Ti–10Zr–5Ta–5Nb$_{tt}$ alloy substrate was comparable to that of cells cultured on plastic substrate.

5. On the both studied surfaces, osteoblast adopted a typical morphology with a similar actin expression pattern; a parallel orientation tendency imposed probably by material topography was observed for Ti–10Zr–5Ta–5Nb_{tt} alloy.

Acknowledgment This work was supported by Romanian MEC-CNMP: PN II 07/Contract Number 71-021/2007.

References

1. Thomsen P, Larsson C, Ericson LE, Sennerby L, Lausama J, Kasemo B. Structure of the interface between rabbit cortical bone and implants of gold, zirconium and titanium. J Mater Sci. 1997;8:653–65.
2. Kim H-K, Jang J-W. Surface modification of implant materials and its effect on attachment and proliferation of bone cells. J Mater Sci. 2004;15:825–30.
3. Anselme K, Bigerelle M, Noel B, Dufresne E, Judas D, Iost A, et al. Qualitative and quantitative study of human osteoblast adhesion on materials with various surface roughnesses. J Biomed Mater Res. 2000;49:155–66.
4. Briem D, Strametz S, Schroder K, Meenen NM, Lechmann W, Linhart W, et al. Response of primary fibroblasts and osteoblasts to plasma treated polyetheretherketone (PEEK) surfaces. J Mater Sci. 2005;16:671–7.
5. Mendes SC, Tibbe JM, Veenhof M, Both S, Oner FC, Van Blitterswijk CA, et al. Relation between in vitro and in vivo osteogenic potential of cultured human bone marrow stromal cells. J Mater Sci. 2004;15:1123–8.
6. Miyamoto S, Teramoto H, Coso QA, Gutkind JS, Burbelo PD, Akiyama SK, et al. Integrin function: molecular hierarchies of cytoskeletal and signalling molecules. J Cell Biol. 1995;131:791–805.
7. Boudreau NJ, Jones PL. Extracellular matrix and integrin signalling: the shape of things to come. Biochem J. 1999;339:481–8.
8. Schneider GB, Zaharia R, Stanford C. Osteoblast integrin adhesion and signalling regulate mineralization. J Dent Res. 2001;80:1540–4.
9. Souto RM, Burstein GT. A preliminary investigation into the microscopic depassivation of passive titanium implant materials in vitro. J Mater Sci. 1996;7:337–43.
10. Spriano S, Bronzoni M, Verne E, Maina G, Bergo V, Windler M. Characterization of surface modified Ti-6Al-7Nb alloy. J Mater Sci. 2005;16:301–12.
11. Martins DQ, Osorio WR, Souza EP, Caram R, Garcia A. Effects of Zr content on microstructure and corrosion resistance of Ti-30Nb-Zr casting alloys for biomedical applications. Electrochim Acta. 2008;53:2809–17.
12. Geetha M, Kamachi Mudali U, Gogia AK, Asokamani RE, Raj B. Influence of microstructure and alloying elements on corrosion behaviour of Ti-13Nb-13Zr alloy. Corros Sci. 2004;46:877–92.
13. Lavos-Valereto IC, Wolynec S, Ramires I, Guastaldi AC, Costa I. Electrochemical impedance spectroscopy characterization of passive film formed on implant Ti-6Al-7Nb alloy in Hank's solution. J Mater Sci. 2004;15:55–9.
14. Yu SY, Scully JR. Corrosion and passivity of Ti-13%Nb-13%Zr in comparison to other biomedical implant alloys. Corrosion 1997;53:965–76.
15. Gutierrez A, Lopez MF, Jimenez JA, Morant C, Paszti R, Climent A. Surface characterization of the oxide layer grown on Ti-Nb-Zr and Ti-Nb-Al alloys. Surf Interface Anal. 2004;36:977–80.
16. Zhecheva A, Malino S, Tha W. Surface gas nitrating of Ti-6Al-4 V and Ti-6Al-2Sn-4Zr-2Mo-0.08Si alloys. Z Metallkd. 2003;94:19–24.
17. Trentani L, Pelillo F, Pavesi FC, Ceciliani L, Cetta G, Forlino A. Evaluation of the $TiMo_{12}Zr_6Fe_2$ alloy for orthopaedic implants: in vitro biocompatibility study by using primary human fibroblast and osteoblasts. Biomaterials. 2002;23:2863–9.
18. Nag S, Banerjee R, Stechschulte J, Fraser HL. Comparison of microstructural evolution in Ti-Mo-Zr-Fe and Ti-15Mo biocompatible alloys. J Mater Sci. 2005;16:679–85.
19. Lopez MF, Gutierrez JA, Jimenez JA. In vitro corrosion behaviour of titanium alloys without vanadium. Electrochim Acta. 2002;47:1359–64.
20. Eisenbarth E, Velten D, Mueller M, Thull R, Breme J. Biocompatibility of β-stabilizing elements of titanium alloys. Biomaterials 2004;25:5705–13.
21. Okazaki Y, Nishimura E, Nakada H, Kobaiashi K. Surface analysis of Ti-15Zr-4Nb-4Ta alloy after implantation in rat tibia. Biomaterials. 2001;22:599–607.
22. Okazaki Y. A new Ti-15Zr-4Nb-4Ta alloy for medical application. Curr Opin Solid St M. 2001;5:45–53.
23. Lopez MF, Jimenez JA, Gutierrez A. Corrosion study of surface modified vanadium free titanium alloys. Electrochim Acta. 2003;48:1395–401.
24. Khan MA, Williams RL, Williams DF. In vitro corrosion and wear of titanium alloys in the biological environment. Biomaterials. 1996;17:2117–26.
25. Assis SL, Costa I. Electrochemical evaluation of Ti-13Nb-13Zr, Ti-6Al-4 V and Ti-6Al-7Nb alloys for biomedical application by long-term immersion tests. Mater Corros. 2007;58:329–33.
26. Lopez MF, Soriano L, Palomares FJ, Sanchez-Agudo M, Fuentes GG, Gutierrez A, et al. Soft X-ray absorption spectroscopy study of oxide layers on titanium alloys. Surf Interface Anal. 2002;33:570–6.
27. Morant C, Lopez MF, Gutierrez A, Jimenez JA. AFM and SEM characterization of non-toxic vanadium-free Ti alloys used as biomaterials. Appl Surf Sci. 2003;220:79–87.
28. Tamilselvi S, Rajendran N. In vitro corrosion behaviour of Ti-5Al-2Nb-1Ta alloy in Hank's solution. Mater Corros. 2007;58:285–9.
29. Robin A, Meirelis JP. Influence of fluoride concentration and pH on corrosion behavior of Ti-6Al-4 V and Ti-23Ta alloys in artificial saliva. Mater Corros. 2007;58:173–80.
30. Cai Z, Nakajima N, Woldu M, Berglund A, Bergmon M, Okabe T. In vitro corrosion resistance of titanium made using different fabrication methods. Biomaterials. 1999;20:183–90.
31. Gluszek J, Masalski J, Furman P, Nitsch K. Structural and electrochemical examinations of PACVD TiO_2 films in Ringer solutions. Biomaterials 1997;18:789–94.
32. Popa MV, Demetrescu I, Vasilescu E, Drob P, Santana Lopez A, Mirza-Rosca J, et al. Corrosion susceptibility of implant materials Ti-5Al-4 V and Ti-6Al-4Fe in artificial extra-cellular fluids. Electrochim Acta. 2004;49:2113–9.
33. Popa MV, Demetrescu I, Suh S-H, Vasilescu E, Drob P, Ionita D, et al. Monitoring of titanium base alloys−biofluids interface. Bioelectrochemistry. 2007;71:126–34.
34. Popa MV, Vasilescu E, Drob P, Vasilescu C, Demetrescu I, Ionita D. Long-term assessment of the implant titanium material–artificial saliva interface. J Mater Sci. 2008;19:1–9.
35. Vasilescu E, Drob P, Raducanu D, Dan I, Vasilescu C. Corrosion resistance of some thermo-mechanical treated titanium bioalloy depending on pH of Ringer solution. Rev Chim. (Bucharest). 2009;60:241–7.
36. Van Kesteren IEH. Product designers' information needs in materials selection. Mater Des. 2008;29:133–45.

37. Elias LM, Schneider SG, Schneider S, Silva HM, Malvisi F. Microstructural and mechanical characterization of biomedical Ti–Nb–Zr(–Ta) alloys. Mat Sci Eng A-Struct. 2006;432:108–12.
38. Li S, Xiong B, Hui S, Ye W, Yu Y. Comparison of the fatigue and fracture of Ti–6Al–2Zr–1Mo–1V with lamellar and bimodal microstructures. Mat Sci Eng A Struct. 2007;460–461:140–5.
39. Kima HS, Limb SH, Yeo ID, Kima WY. Stress-induced martensitic transformation of metastable-titanium alloy. Mat Sci Eng A-Struct. 2007;449–451:322–5.
40. Popa MV, Raducanu D, Vasilescu E, Drob P, Cojocaru VD, Vasilescu C, et al. Mechanical and corrosion behaviour of a Ti-Al-Nb alloy after deformation at elevated temperatures. Mater Corros. 2008;59:919–28.
41. Gordin DM, Gloriant T, Texier G, Thibon I, Ansel D, Duval JL, et al. Development of a β-type Ti-12Mo-5Ta alloy for biomedical applications: cytocompatibility and metallurgical aspects. J Mater Sci. 2004;15:885–91.
42. Bastos AC, Somoes AM, Gonzalez S, Gonzalez-Garcia Y, Souto RM. Imaging concentration profiles of redox-active species in open-circuit corrosion processes with the scanning electron microscope. Electrochem Commun. 2004;6:1212–5.
43. Souto RM, Laz MM, Reis RL. Degradation characteristics of hydroxyapatite coatings on orthopaedic TiAlV in simulated physiological media investigated by electrochemical impedance spectroscopy. Biomaterials. 2003;24:4213–21.
44. Pourbaix M. Atlas of electrochemical equilibria in aqueous solutions. Houston, TX: NACE;1974. p. 213–221, 223–229, 246–250 and 251–255.
45. ISO TR 10271:2001, Dental metallic materials – Corrosion test methods.
46. Thomson NG, Buchanan RA, Lemons JE. In vitro corrosion of Ti-6Al-4 V and type 316L stainless steel when gallvanically coupled with carbon. J Biomed Mater Res. 1979;13:35–44.
47. Shlaby LA. Galvanic coupling of Ti with Cu and Al alloys in chloride media. Corros Sci. 1971;11:767–78.
48. Guo OK, Du M, Zhou CJ. Study of galvanic corrosion of carbon steel/titanium and carbon steel/titanium/navel brass in seawater. *In*: Proceedings of 16th International Corrosion. 1–8, September 2005, Beijing, China, Ed. International Corrosion Council, paper 11–3.
49. Thian S, Huang J, Best SM, Barber ZH, Brooks RA, Rushton N, et al. The response of osteoblasts to nanocrystalline silicon-substituted hydroxyapatite thin films. Biomaterials. 2006;27:2692–8.
50. Prado Da Silva MH, Soares GDA, Elias CN, Best SM, Gibson IR, Di Silvio L, et al. In vitro cellular response of titanium electrochemically coated with hydroxyapatite compared to titanium with three different levels of surface roughness. J Mater Sci. 2003;14:511–9.
51. Navarro M, Ginebra MP, Planell JA. Cellular response to calcium phosphate glasses with controlled solubility. J Biomed Mater Res. A. 2004;67:1009–15.
52. Hynes RO. Integrins: versatility, modulation and signaling in cell adhesion. Cell. 1992;69:11–25.
53. Giancotti FG, Ruoslahti E. Integrin signals. Science. 1999;285:1028–31.
54. Rea SM, Brooks RA, Schneider A, Best SM, Bonfield W. Osteoblast-like cell response to bioactive composites-surface-topography and composition effects. J Biomed Mater Res. B. 2004;70:250–61.
55. Milosev I, Kosec T, Strehblow H-H. XPS and EIS study of the passive film formed on orthopaedic Ti-6Al-7Nb alloy in Hank's physiological solution. Electrochim Acta. 2008;53:3547–58.
56. Black J. Biological performance of materials: fundamentals of biocompatibility. New York: Decker M Inc; 1992.
57. Blackwood DJ, Chua AWC, Seah KHW, Thampuran R, Teoh SH. Corrosion behaviour of porous titanium-graphite composites designed for surgical implants. Corros Sci. 2003;42:481–503.